Spontaneous decay rate and Casimir-Polder potential of an atom near a lithographed surface

Robert Bennett*
Department of Physics & Astronomy, University of Leeds, Leeds LS2 9JT, United Kingdom
(Received 11 April 2015; published 10 August 2015)

Radiative corrections to an atom are calculated near a half-space that has arbitrarily shaped small depositions upon its surface. The method is based on calculation of the classical Green's function of the macroscopic Maxwell equations near an arbitrarily perturbed half-space using a Born-series expansion about the bare half-space Green's function. The formalism of macroscopic quantum electrodynamics is used to carry this over into the quantum picture. The broad utility of the calculated Green's function is demonstrated by using it to calculate two quantities: the spontaneous decay rate of an atom near a sharp surface feature and the Casimir-Polder potential of a finite grating deposited on a substrate. Qualitatively different behavior is found for the latter case where it is observed that the periodicity of the Casimir-Polder potential persists even outside the immediate vicinity of the grating.

DOI: 10.1103/PhysRevA.92.022503 PACS number(s): 31.30.jh, 12.20.Ds, 34.35.+a, 42.50.Ct

I. INTRODUCTION

Quantum fluctuations of the electromagnetic (EM) field are influenced by material boundaries, meaning that a wide variety of quantum electrodynamical vacuum quantities have an environment dependence. These effects are often referred to as dispersion forces. Famous examples include the force between macroscopic objects known as the Casimir effect [1], and the closely related Casimir-Polder (CP) force [2] between an atom and a surface. Other examples include modified spontaneous decay rates (see, for example, [3–6]), magnetic moments [7–13], cyclotron frequencies [11,14], and Zeeman splittings [15,16].

There is contemporary interest in how dispersion forces are modified by the specifics of the surfaces involved. This can be by consideration of their optical properties [17], their thermal environment [18], or their geometries. An example of the latter is found in [19], where it is shown that nontrivial geometry-dependent vacuum effects can be studied by using a Bose-Einstein condensate above a corrugated surface. Dispersion-force calculations that go beyond simple planar geometries are usually complicated in the extreme due to the inherent nonadditivity of dispersion forces (see, for example, [20] and [21]). To remedy this, various simplifying approaches have been developed, one of the most prominent being the *proximity-force approximation* (PFA) [22], where one models complex geometries as made up of an ensemble of flat, parallel surfaces. It has been shown repeatedly both in theory [23–29] and in experiment [30,31] that the PFA is uncontrolled and is often significantly in error. Alternative theoretical approaches are based around at least one of the following assumptions: the surface having stochastic roughness or being "almost smooth" [23,24,32,33], being periodic [25–27] and thus allowing the calculation to take advantage of the Bloch theorem, or being specialized to a particular quantity (such as atomic decay rates, as done in [34], for example). However, no general treatment of arbitrarily shaped (nonperiodic, nonstochastic) mechanically etched surfaces with sharp edges like those discussed in [35] has yet been supplied.

Here we use a method based on the Born expansion of the Green's function of the EM wave equation to calculate environment-modified decay rates and CP potentials near a selection of geometries. In contrast to the PFA, this approach preserves the rich geometry dependence of dispersion forces, at the expense of requiring the system to consist of a small "geometric perturbation" from an exactly solvable "background" geometry. This approach has been used before in the calculation of CP potentials [36] and Casimir forces [37,38] and is familiar from physical optics (see, for example, [39]) One of the main differences between our work and [36–38] is that only homogeneous backgrounds were considered there, while we consider a half-space as the background. The advantage of this is that the optical properties of the half-space can be specified completely freely: it is not part of the perturbation so its electromagnetic response does not need to satisfy any of the conditions that ensure convergence of the perturbation series. This allows one to make perturbative calculations for quantum electrodynamical quantities near arbitrarily shaped small depositions onto the surface of the (nonperturbative) half-space, which is the goal of this paper. These kinds of geometries are relevant to very recent experiments on decay rates near patterned materials [40] and are common in studies of surface roughness (e.g., [24] and [4–46]), but as explained later, these roughness works make additional assumptions which we do not make here.

II. THEORETICAL BACKGROUND

We use the noise-current approach [47–49] to EM field quantization in and around dielectric media. This approach is necessitated by the fact that Maxwell's equations in a dispersive, absorbing medium cannot be quantized simply by promoting the field observables to operators, as this would cause a violation of the fluctuation-dissipation theorem. To remedy this, one introduces a source current density operator $\mathbf{j}$ which corresponds to noise associated with loss in the medium and restores consistency with the fluctuation-dissipation theorem [48–51]. It is interesting to note that in its original form this theory did not rest on a rigorous canonical foundation, however, this was recently remedied in [52]. The advantage of the use of this source current representation is that it allows the quantised field to be obtained from the classical Green's function for the EM field in a given configuration [48–51]. In this framework, the frequency-domain *quantized* electric field

*r.bennett@leeds.ac.uk

that solves Maxwell's equations in a medium with position- and frequency-dependent permittivity $\epsilon(\mathbf{r},\omega)$ is given by the solution to the wave equation [53]

$$\nabla \times \nabla \times \mathbf{E}(\mathbf{r},\omega) - \omega^2 \epsilon(\mathbf{r},\omega)\mathbf{E}(\mathbf{r},\omega) = i\omega \mathbf{j}(\mathbf{r},\omega), \quad (1)$$

with $\mathbf{j}$ being the operator-valued noise-current source discussed above. This can be solved by the introduction of a Green's function (variously called the dyadic Green's function or the Green's tensor) [48,49] which we call $\mathbf{W}(\mathbf{r},\mathbf{r}',\omega)$ [54]. It is defined as the solution to

$$\nabla \times \nabla \times \mathbf{W}(\mathbf{r},\mathbf{r}',\omega) - \omega^2 \epsilon(\mathbf{r},\omega)\mathbf{W}(\mathbf{r},\mathbf{r}',\omega) = \mathbb{I}\delta(\mathbf{r}-\mathbf{r}'), \quad (2)$$

where $\mathbb{I}$ is a 3×3 unit matrix.

The Green's function $\mathbf{W}$ defined by (2) uniquely determines the quantized field in a particular configuration, which ultimately means that knowledge of $\mathbf{W}$ allows one to calculate a wide variety of quantum electrodynamical quantities [55]. However, exact calculation of the Green's function $\mathbf{W}$ is only possible analytically for the very simplest choices of $\epsilon(\mathbf{r},\omega)$, so here we avoid this problem by using a perturbative technique. As shown in [36] one can write the unknown $\mathbf{W}$ in terms of some known "background" Green's function $\mathbf{W}^{(0)}(\mathbf{r},\mathbf{r}',\omega)$ as

$$\begin{aligned}\mathbf{W}(\mathbf{r},\mathbf{r}',\omega) &= \mathbf{W}^{(0)}(\mathbf{r},\mathbf{r}',\omega) \\ &+ \omega^2 \int d^3\mathbf{s}_1 \mathbf{W}^{(0)}(\mathbf{r},\mathbf{s}_1,\omega)\delta\epsilon(\mathbf{s}_1,\omega)\mathbf{W}^{(0)}(\mathbf{s}_1,\mathbf{r}',\omega) \\ &+ \omega^4 \int d^3\mathbf{s}_1 \int d^3\mathbf{s}_2 [\mathbf{W}^{(0)}(\mathbf{r},\mathbf{s}_1,\omega)\delta\epsilon(\mathbf{s}_1,\omega) \\ &\times \mathbf{W}^{(0)}(\mathbf{s}_1,\mathbf{s}_2,\omega)\delta\epsilon(\mathbf{s}_2,\omega)\mathbf{W}^{(0)}(\mathbf{s}_2,\mathbf{r}',\omega)] + \ldots, \end{aligned} \quad (3)$$

where $\delta\epsilon(\mathbf{r},\omega)$ is the difference between the entire dielectric function and that of the background material at a particular point $\mathbf{r}$. Throughout this work we use the superscript (0) to refer to the known background part of a particular Green's function. This type of perturbative expansion is known as the Born series and is the foundation of much of scattering theory: the spatial integrations over $\mathbf{s}_i$ have a definite interpretation as scattering events [36–38,51].

We can simplify the Born series, (3), by specifying that the configurations we are interested in are always made up of an object described by some volume $\mathbf{V}$ that has an internally homogeneous dielectric function, $\epsilon(\mathbf{r},\omega) = \epsilon(\omega)$, and sits in some (possibly inhomogeneous) background material with dielectric function $\epsilon^{(0)}(\mathbf{r},\omega)$. Under these assumptions we can restrict the $\mathbf{s}_i$ integrals to being over the volume $\mathbf{V}$, because outside this region the background dielectric function at a particular point is equal to the entire dielectric function at that point, so $\delta\epsilon(\mathbf{r},\omega) = 0$ there. The assumption of homogeneity within the volume $\mathbf{V}$ means we can also bring the dielectric functions outside the integrals, giving

$$\begin{aligned}\mathbf{W}(\mathbf{r},\mathbf{r}',\omega) &= \mathbf{W}^{(0)}(\mathbf{r},\mathbf{r}',\omega) \\ &+ \omega^2[\delta\epsilon(\omega)] \int_{\mathbf{V}} d^3\mathbf{s}_1 \mathbf{W}^{(0)}(\mathbf{r},\mathbf{s}_1,\omega)\mathbf{W}^{(0)}(\mathbf{s}_1,\mathbf{r}',\omega) \\ &+ \omega^4[\delta\epsilon(\omega)]^2 \int_{\mathbf{V}} d^3\mathbf{s}_1 \int_{\mathbf{V}} d^3\mathbf{s}_2 [\mathbf{W}^{(0)}(\mathbf{r},\mathbf{s}_1,\omega) \\ &\times \mathbf{W}^{(0)}(\mathbf{s}_1,\mathbf{s}_2,\omega)\mathbf{W}^{(0)}(\mathbf{s}_2,\mathbf{r}',\omega)] + \ldots. \end{aligned} \quad (4)$$

This type of approach has been used before in studies of surface roughness. For example, a similar relation appears in [42], but for the electric field rather than the Green's function. As mentioned in Sec. I, the work presented here differs from [42] for a number of reasons, chief among them being that we are not considering roughness so cannot use its stochastic properties to simplify calculations.

In order to work out surface-modified quantities we need the so-called "scattering" part of the Green's function, (4)—that is, the part which remains after the point-by-point subtraction of the Green's function for a homogeneous region. In other words, to find the scattering Green's function one takes the *whole* Green's function and then at each point in space subtracts the Green's function for a homogeneous region with the same permittivity as the point in question. We write the scattering part of the Green's function $\mathbf{W}$ as $\mathbf{G}$ and the remaining part as $\mathbf{H}$. This means that the whole Green's function can be rewritten

$$\begin{aligned}\mathbf{W}(\mathbf{r},\mathbf{r}',\omega) &= \mathbf{G}^{(0)}(\mathbf{r},\mathbf{r}',\omega) + \mathbf{H}^{(0)}(\mathbf{r},\mathbf{r}',\omega) \\ &+ \omega^2[\delta\epsilon(\omega)] \int_{\mathbf{V}} d^3\mathbf{s}_1 [\mathbf{G}^{(0)}(\mathbf{r},\mathbf{s},\omega) + \mathbf{H}^{(0)}(\mathbf{r},\mathbf{s},\omega)] \\ &\cdot [\mathbf{G}^{(0)}(\mathbf{s},\mathbf{r}',\omega) + \mathbf{H}^{(0)}(\mathbf{s},\mathbf{r}',\omega)] + \ldots. \end{aligned} \quad (5)$$

In previous calculations [36–38] the background Green's function $\mathbf{W}^{(0)}$ was taken to be that for a homogeneous medium, so that its scattering part $\mathbf{G}^{(0)}$ is, by definition, 0. This has the simplifying property that the partitioning of the Green's function via the Born series coincides with the partitioning one makes when finding the scattering part; i.e., for homogeneous $\mathbf{H}$

$$\begin{aligned}\mathbf{W}_{\mathbf{H}\,\mathrm{hom}}(\mathbf{r},\mathbf{r}',\omega) &= \mathbf{H}^{(0)}(\mathbf{r},\mathbf{r}',\omega) + \omega^2[\delta\epsilon(\omega)] \\ &\times \int_{\mathbf{V}} d^3\mathbf{s}_1 \mathbf{H}^{(0)}(\mathbf{r},\mathbf{s},\omega)\mathbf{H}^{(0)}(\mathbf{s},\mathbf{r}',\omega), \end{aligned} \quad (6)$$

meaning that the scattering part is

$$\begin{aligned}&\mathbf{G}_{\mathbf{H}\,\mathrm{hom}}(\mathbf{r},\mathbf{r}',\omega) \\ &= \omega^2[\delta\epsilon(\omega)] \int_{\mathbf{V}} d^3\mathbf{s}_1 \mathbf{H}^{(0)}(\mathbf{r},\mathbf{s},\omega)\mathbf{H}^{(0)}(\mathbf{s},\mathbf{r}',\omega). \end{aligned} \quad (7)$$

This means that all that is required for the calculation of environment-dependent quantities in a geometry regarded as a perturbation to a *homogeneous* medium is an integral over a homogeneous Green's function, which is relatively simple to do. However, this is not usually a case of physical interest since in real experiments there will likely be an object nearby that does not obey the conditions for convergence that the Born expansion requires. To remedy this, we study the simplest *inhomogeneous* background, namely, a half-space, and then add perturbing objects to *that*, as shown in Fig. 1. This type of approach has long been used in the study of EM scattering from rough surfaces (see, for example, [24] and [41–44],), however, these calculations usually rely on the specific stochastic properties of the roughness in order to simplify calculations. This is not done here: the surface additions are allowed to be arbitrary.

In this work we truncate the Born series at the single-scattering term, though it is straightforward to extend the method to higher-order terms as is required to work out Casimir forces [38], as opposed to decay rates and CP potentials as

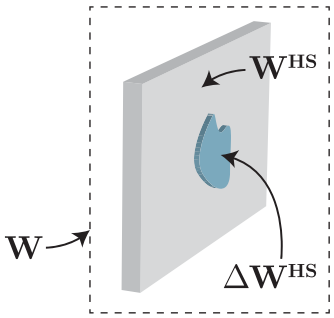

FIG. 1. (Color online) General setup.

done here. We then have the whole Green's function to order $\delta\epsilon(\mathbf{r},\omega)$,

$$\begin{aligned}\mathbf{W}(\mathbf{r},\mathbf{r}',\omega) &= \mathbf{W}^{\mathrm{HS}}(\mathbf{r},\mathbf{r}',\omega)\\ &\quad+\omega^2[\delta\epsilon(\omega)]\int_V d^3\mathbf{s}\mathbf{W}^{\mathrm{HS}}(\mathbf{r},\mathbf{s},\omega)\mathbf{W}^{\mathrm{HS}}(\mathbf{s},\mathbf{r}',\omega)\\ &= \mathbf{W}^{\mathrm{HS}}(\mathbf{r},\mathbf{r}',\omega)+\Delta\mathbf{W}^{\mathrm{HS}}(\mathbf{r},\mathbf{r}',\omega),\end{aligned}\tag{8}$$

with $\mathbf{W}^{\mathrm{HS}}$ being the Green's function for a half-space. A similar relation for the electric field (rather than the Green's function) appears in the surface-roughness literature, for example, in [42]. The half-space Green's function at frequency ω in a region $z>0$ in the presence of a nonmagnetic material half-space filling the region $z<0$ is conveniently written as [56]

$$\begin{aligned}\mathbf{W}^{\mathrm{HS}}(\mathbf{r},\mathbf{r}',\omega) &= -\frac{\hat{z}\otimes\hat{z}}{k^2}\delta(\mathbf{r}-\mathbf{r}')\\ &\quad+\frac{i}{8\pi^2}\sum_\sigma\int d^2\mathbf{k}_\parallel\frac{\mathcal{D}_\sigma(\mathbf{r},\mathbf{r}')}{k_\parallel^2 k_z}\\ &\quad\times e^{i\mathbf{k}_\parallel\cdot(\mathbf{r}_\parallel-\mathbf{r}'_\parallel)}F^\sigma_\pm(z,z'),\end{aligned}\tag{9}$$

where $k_z\equiv\sqrt{\omega^2-k_\parallel^2}$ and $\mathbf{r}_\parallel$ and $\mathbf{k}_\parallel$ are, respectively, the components of the position and wave vector parallel and perpendicular to the interface, and $\hat{z}$ is a unit vector perpendicular to the interface. The symbol σ indexes the two possible polarizations [TE (transverse electric) and TM (transverse magnetic)] of the Coulomb-gauge EM field, and $\mathcal{D}_\sigma$ represents the following differential operators:

$$\begin{aligned}\mathcal{D}_{\mathrm{TE}}(\mathbf{r},\mathbf{r}') &\equiv (\nabla\times\hat{z})\otimes(\nabla'\times\hat{z}),\\ \mathcal{D}_{\mathrm{TM}}(\mathbf{r},\mathbf{r}') &\equiv \frac{1}{\omega^2}(\nabla\times\nabla\times\hat{z})\otimes(\nabla'\times\nabla'\times\hat{z}).\end{aligned}\tag{10}$$

Finally, the function $F^\sigma_\pm(z,z')$ is given by

$$F^\sigma(z,z')=[e^{-ik_z\mathcal{Z}_<}+e^{ik_z\mathcal{Z}_<}R^\sigma_{vm}]e^{ik_z\mathcal{Z}_>},\tag{11}$$

where $\mathcal{Z}_>$ is the greater of z and z', and $\mathcal{Z}_<$ is the lesser of z and z';

$$\mathcal{Z}_>=\begin{cases}z & \text{for}\quad z>z',\\ z' & \text{for}\quad z<z',\end{cases}\qquad \mathcal{Z}_<=\begin{cases}z' & \text{for}\quad z>z',\\ z & \text{for}\quad z<z'\end{cases}\tag{12}$$

and R^σ_{vs} are the Fresnel coefficients for radiation propagating from a vacuum region into a medium of permittivity $\epsilon(\omega)$

$$R^{\mathrm{TE}}_{vm}=\frac{k_z-k_z^d}{k_z+k_z^d},\qquad R^{\mathrm{TM}}_{vm}=\frac{\epsilon(\omega)k_z-k_z^d}{\epsilon(\omega)k_z+k_z^d},\tag{13}$$

where $k_z^d=\sqrt{\epsilon(\omega)\omega^2-k_\parallel^2}$ is the z component of the wave vector inside the medium. We can now use this statement of the half-space Green's function to generate the next-to-leading-order term $\Delta\mathbf{W}^{\mathrm{HS}}(\mathbf{r},\mathbf{r}',\omega)$ in the Born expansion, (8), which will give the modified Green's function for the EM field in the vicinity of a half-space with depositions.

III. MODIFIED GREEN'S FUNCTION

We now present the Green's function modification $\Delta\mathbf{W}^{\mathrm{HS}}(\mathbf{r},\mathbf{r}',\omega)$ for a half-space with a deposition. We restrict ourselves to the region $\mathbf{r},\mathbf{r}'\neq\mathbf{s}$ throughout this work, meaning that we can ignore the δ function terms in (9) when substituting it into (8). This means that we do not calculate any quantum electrodynamical quantities *inside* a deposition onto a half-space. Apart from complicating the method used here, calculation of such quantities would require the use of local-field-corrected Green's tensors [6,57,58], which are beyond the scope of this work. Under these assumptions, we note that $\Delta\mathbf{W}(\mathbf{r},\mathbf{r}',\omega)$ depends quadratically on F^σ, so from the form of Eq. (11) one sees that that all contributions to $\Delta\mathbf{W}$ as defined in Eq. (8) must be at most quadratic in the reflection coefficients, so we can write

$$\begin{aligned}\Delta\mathbf{W}^{\mathrm{HS}}_{ij}(\mathbf{r},\mathbf{r}',\omega) &= \int_{\mathbf{V}}d^3\mathbf{s}\int d^2\mathbf{k}_\parallel\int d^2\mathbf{k}'_\parallel P\\ &\quad\times\Bigg[1+K^{\mathrm{TETM}}_{ij\lessgtr}R_{\mathrm{TE}}R_{\mathrm{TM}}\\ &\quad+\sum_\sigma\left(K^\sigma_{ij\lessgtr}R_\sigma+K^{\sigma\sigma}_{ij\lessgtr}R_\sigma^2\right)\Bigg],\end{aligned}\tag{14}$$

where, for later convenience, we have defined the quantity P as

$$\begin{aligned}P &= -\frac{\delta\epsilon(\omega)}{64\pi^4\omega^4k_\parallel^2k_\parallel'^2k_zk_z'}\exp\{i[\mathbf{k}_\parallel\cdot(\mathbf{r}_\parallel-\mathbf{s}_\parallel)\\ &\quad+\mathbf{k}'_\parallel\cdot(\mathbf{s}_\parallel-\mathbf{r}'_\parallel)+k_z(r_z+s_z)+k'_z(r'_z+s_z)]\}.\end{aligned}\tag{15}$$

The various $K_{ij\lessgtr}$ in (14) are matrix elements determined from Eqs. (8) and (9) by simple but tedious application of the differential operators, (10), to the functions $F^\sigma_\pm(z,z')$ defined in Eq. (11). The matrix elements differ depending on whether r_z is greater or less than s_z; the subscript $\lessgtr$ distinguishes these two cases, as detailed in the full list of matrix elements given in the Appendix.

A. Simple demonstration: Decay rate near a sharp surface feature

We, begin with a surface-modified quantity that is relatively easy to calculate, namely the spontaneous decay rate of an excited atom that is attributable to its interaction with the quantized EM field. The effect of the surface geometry on this rate has been measured [59], and similar calculations find applications in near-field optical microscopy [60–62]. Theoretical predictions of the decay rate near surface depositions have been made before using techniques similar to those presented here [34,63]; its calculation is included in this work as an example to illustrate the method.

It is well known (see, for example, [4] and [64]) that the decay rate Γ can be expressed in terms of the Green's function $\mathbf{W}$ as

$$\Gamma = 2\omega_A^2 \mathbf{d}\cdot[\mathrm{Im}\mathbf{W}(\mathbf{r}_A,\mathbf{r}_A,\omega_A)]\cdot\mathbf{d}^*, \tag{16}$$

where $\mathbf{d}$ is the dipole moment of the transition. As a demonstrative example we present a calculation of the decay rate Γ_0 of an atom in vacuum, with no material objects present. We can choose the direction of the polarization freely because in vacuum we have rotation invariance; we choose the polarization to be aligned along the $\mathbf{z}$ direction so that $\mathbf{d} = d\hat{\mathbf{z}}$. Then

$$\Gamma_0 = 2\omega_A^2|d|^2\mathrm{Im}\mathbf{W}^{\mathrm{vac}}_{zz}(\mathbf{r}_A,\mathbf{r}_A,\omega_A), \tag{17}$$

where $\mathbf{W}^{\mathrm{vac}}_{zz}$ is the zz component of the Green's function that solves (2) for $\epsilon(\mathbf{r},\omega) = 1$. This vacuum Green's function is well known (see [51] for a thorough review). It can be found, for example, from the half-space Green's function, (9), reported here by taking all reflection coefficients to 0:

$$\mathbf{W}^{\mathrm{vac}}(\mathbf{r},\mathbf{r}',\omega) = \mathbf{W}^{\mathrm{HS}}(\mathbf{r},\mathbf{r}',\omega)|_{R^\sigma=0}. \tag{18}$$

The zz component of the vacuum Green's function is

$$\mathbf{W}^{\mathrm{vac}}_{zz}(\mathbf{r},\mathbf{r}',\omega_A) = \frac{i}{8\pi^2}\int d^2\mathbf{k}_\parallel \frac{k_\parallel^2}{\omega^2 k_z} e^{ik_z|z-z'|}, \tag{19}$$

where we have ignored the (real-valued) δ function part of (9) in anticipation of taking the imaginary part as dictated by (16). Transforming to polar coordinates in the k_x,k_y plane and doing the trivial angular integral, we have

$$\mathbf{W}^{\mathrm{vac}}_{zz}(\mathbf{r},\mathbf{r}',\omega_A) = \frac{i}{4\pi}\int_0^\infty dk_\parallel \frac{k_\parallel^3}{\omega^2 k_z} e^{ik_z|z-z'|}. \tag{20}$$

The integral can be carried out analytically, giving

$$\mathbf{W}^{\mathrm{vac}}_{zz}(\mathbf{r},\mathbf{r}',\omega_A) = \frac{1}{2\pi\omega^2}\frac{e^{i\omega|z-z'|}}{|z-z'|^3}(1-i\omega|z-z'|). \tag{21}$$

Taking the imaginary part of this followed by the coincidence limit $z' \to z$, we find, upon substitution into (17),

$$\Gamma_0 = \frac{\omega_A^3}{3\pi}|d|^2, \tag{22}$$

which is a well-known result (see, for example, [65]) and is used as a convenient unit in the following discussions.

As another point of comparison we also present the known results for the decay rate near a half-space [4,66],

$$\Gamma^{\mathrm{HS}} = 2\omega_A^2 \mathbf{d}\cdot[\mathrm{Im}\mathbf{W}^{\mathrm{HS}}(\mathbf{r}_A,\mathbf{r}_A,\omega_A)]\cdot\mathbf{d}^*,$$

which we split into the free-space contribution Γ_0 and a surface-modified part $\Delta\Gamma^{\mathrm{HS}}$:

$$\begin{aligned}\Gamma^{\mathrm{HS}} &= 2\omega_A^2\mathbf{d}\cdot[\mathrm{Im}(\mathbf{W}_{\mathrm{vac}}(\mathbf{r}_A,\mathbf{r}_A,\omega_A)+\mathbf{G}^{\mathrm{HS}}(\mathbf{r}_A,\mathbf{r}_A,\omega_A)]\cdot\mathbf{d}^*\\ &= \frac{\omega_A^3|d^2|}{3\pi} + 2\omega_A^2\mathbf{d}\cdot\mathrm{Im}\mathbf{G}^{\mathrm{HS}}(\mathbf{r}_A,\mathbf{r}_A,\omega_A)\cdot\mathbf{d}^*\\ &= \Gamma_0 + \Delta\Gamma^{\mathrm{HS}}.\end{aligned} \tag{23}$$

We consider the two cases where the atom is polarized parallel and perpendicular to the surface with the same magnitude of dipole moment $d = |\mathbf{d}|$ and separately find the two contributions $\Delta\Gamma^{\mathrm{HS}}_\parallel$ and $\Delta\Gamma^{\mathrm{HS}}_\perp$ to the decay rates $\Gamma_\parallel = \Gamma_0 + \Delta\Gamma^{\mathrm{HS}}_\parallel$ and $\Gamma_\perp = \Gamma_0 + \Delta\Gamma^{\mathrm{HS}}_\perp$. Calculation of $\Delta\Gamma^{\mathrm{HS}}_\parallel$ is simplified by exploiting invariance in the xy plane to assume without loss of generality that the dipole in this case is aligned along the x direction. Therefore we need to calculate

$$\Delta\Gamma^{\mathrm{HS}}_\parallel = 2\omega_A^2|d|^2\mathrm{Im}\mathbf{G}^{\mathrm{HS}}_{xx}(\mathbf{r}_A,\mathbf{r}_A,\omega_A), \tag{24}$$

$$\Delta\Gamma^{\mathrm{HS}}_\perp = 2\omega_A^2|d|^2\mathrm{Im}\mathbf{G}^{\mathrm{HS}}_{zz}(\mathbf{r}_A,\mathbf{r}_A,\omega_A). \tag{25}$$

Using the half-space Green's function, (9), we find

$$\begin{aligned}\mathbf{G}^{\mathrm{HS}}_{zz}(\mathbf{r},\mathbf{r}',\omega_A) &= \frac{i}{4\pi}\int_0^\infty dk_\parallel \frac{k_\parallel^3}{\omega^2 k_z} e^{ik_z(z-z')} R_{\mathrm{TM}} e^{2ik_z z'},\\ \mathbf{G}^{\mathrm{HS}}_{xx}(\mathbf{r},\mathbf{r}',\omega_A) &= \frac{i}{8\pi}\int_0^\infty dk_\parallel \frac{k_\parallel}{\omega^2 k_z} e^{ik_z(z-z')}\\ &\quad\times e^{2ik_z z'}\left(\omega^2 R_{\mathrm{TE}} - k_z^2 R_{\mathrm{TM}}\right).\end{aligned} \tag{26}$$

Substituting these into Eqs. (24) and (25) and evaluating the integrals in the same way as for the free-space case, one eventually finds the following results for the decay rates near a perfect conductor ($R_{\mathrm{TE}} \to -1$, $R_{\mathrm{TM}} \to 1$),

$$\Delta\Gamma^{\mathrm{HS}}_\parallel = \frac{|d|^2}{16\pi z^3}\left[\left(1-4\omega_A^2 z^2\right)\sin(2\omega_A z) - 2\omega_A z\cos(2\omega_A z)\right], \tag{27}$$

$$\Delta\Gamma^{\mathrm{HS}}_\perp = \frac{|d|^2}{8\pi z^3}[\sin(2\omega_A z) - 2\omega_A z\cos(2\omega_A z)], \tag{28}$$

in agreement with [4] and [66]. The z dependence of $\Gamma^{\mathrm{HS}}_\parallel$ and $\Gamma^{\mathrm{HS}}_\perp$ is shown in Fig. 2. This shows the well-known property that an atom whose dipole moment is aligned perpendicular to a perfectly reflecting surface has its decay rate enhanced by a factor of 2 in the small-distance limit. Similarly, an atom whose dipole moment is aligned parallel to such a surface has its decay rate completely suppressed as it approaches the boundary. Far away from the surface the free-space value is recovered in both cases as expected.

We now use our modified Green's function, (14), to produce new results for more complicated geometries, using the above known results as points of comparison. The new geometry that we choose is a cube of side a and refractive index $\epsilon_c(\omega)$ deposited on a half-space, as shown in Fig. 3. This means that

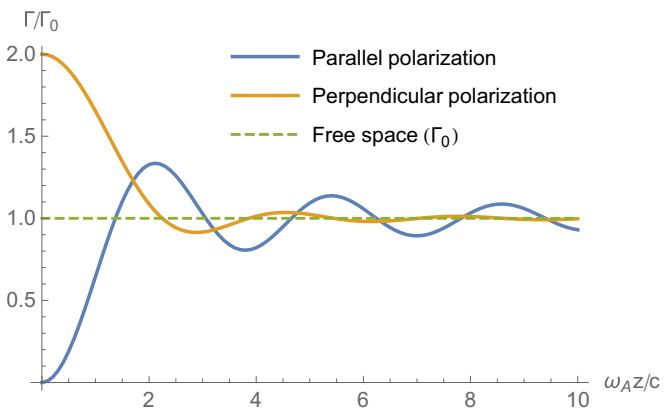

FIG. 2. (Color online) Decay rates near a simple half-space.

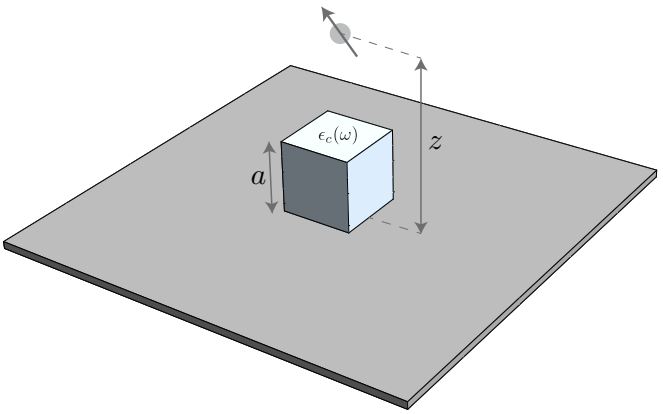

FIG. 3. (Color online) Cubic deposition geometry. The cube and substrate can be made of different materials; the only restriction on their properties is that the cube material must be weakly dielectric in order for the Born series to converge. We emphasize that the substrate can be made of any desired material since it does not take part in the perturbative approximation.

the volume integral over $\mathbf{s}$ in Eq. (14) becomes

$$\int_V d^3\mathbf{s} \to \int_{-a/2}^{a/2} ds_x \int_{-a/2}^{a/2} ds_x \int_0^a ds_z. \tag{29}$$

Part of the reason for choosing this shape in particular is that, as mentioned in Sec. I, the method presented here does not break down for geometries with sharp corners, in contrast to other approaches to radiative corrections near perturbed half-spaces, which rely on the surface being smooth in some sense [32,33]. As we see later, the approach used here can produce highly nontrivial results in the regions near sharp objects.

Taking the modified Green's function, (14), and transforming to polar coordinates $\{k_x,k_y\} = \{k_\parallel \sin\phi, k_\parallel \cos\phi\}$ (with similar definitions for the primed coordinates), we find, for the xx and zz components of the modified Green's function in the limit where the substrate is perfectly reflecting,

$$\begin{aligned}
&\Delta\mathbf{W}^{\text{cube}}_{\text{PM},xx}(\mathbf{r},\mathbf{r}',\omega) \\
&= \frac{\delta\epsilon_c(\omega)}{16\pi^4}\int_0^\infty dk_\parallel \int_0^\infty dk'_\parallel \int_0^{2\pi} d\phi \int_0^{2\pi} d\phi' \\
&\times \frac{k_\parallel k'_\parallel}{\omega^2 k_z k'_z}\frac{k_z\cos(ak_z)\sin(ak'_z) - k'_z\sin(ak_z)\cos(ak'_z)}{(k_\parallel^2 - k_\parallel'^2)(\chi k_\parallel - \chi' k'_\parallel)(\eta k_\parallel - \eta' k'_\parallel)} \\
&\times [(\chi^2 - \eta^2 - 1)k_\parallel^2 + 2\omega^2]\sin[a/2(\chi k_\parallel - \chi' k'_\parallel)] \\
&\times [(\chi'^2 - \eta'^2 - 1)k_\parallel'^2 + 2\omega^2]\sin[a/2(\eta k_\parallel - \eta' k'_\parallel)] \\
&\times e^{i[x(\eta k_\parallel - \eta' k'_\parallel) + y(\chi k_\parallel - \chi' k'_\parallel) + k_z z + k'_z z']}
\end{aligned} \tag{30}$$

and

$$\begin{aligned}
&\Delta\mathbf{W}^{\text{cube}}_{\text{PM},zz}(\mathbf{r},\mathbf{r}',\omega) \\
&= \frac{\delta\epsilon_c(\omega)}{4\pi^4}\int_0^\infty dk_\parallel \int_0^\infty dk'_\parallel \int_0^{2\pi} d\phi \int_0^{2\pi} d\phi' \\
&\times \frac{k_\parallel^3 k_\parallel'^3}{\omega^2 k_z k'_z}\frac{k_z\sin(ak_z)\cos(ak'_z) - k'_z\cos(ak_z)\sin(ak'_z)}{(k_\parallel^2 - k_\parallel'^2)(\chi k_\parallel - \chi' k'_\parallel)(\eta k_\parallel - \eta' k'_\parallel)}
\end{aligned}$$

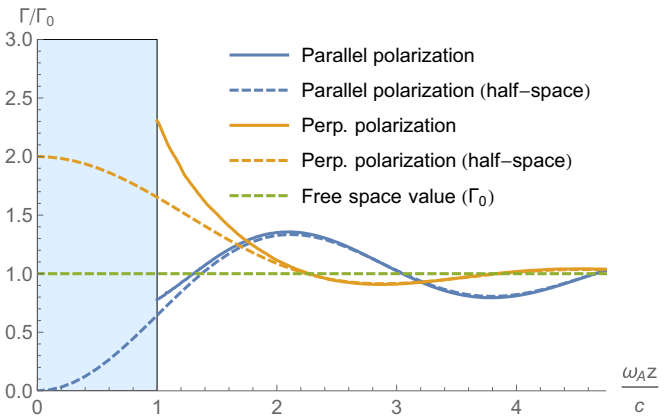

FIG. 4. (Color online) Modified decay rates (solid lines) near a cube of dielectric constant $\epsilon_c(\omega_A) = 1.8$ deposited on a perfectly reflecting half-space, with the decay rates for the bare half-space and free space (dashed lines) shown for comparison. The shaded area represents the depth of the cube added to the half-space. We do not present results for the region interior to the cube because local field effects [6,57,58] would come into play there, but these are beyond the scope of this work.

$$\begin{aligned}
&\times \sin[a/2(\chi k_\parallel - \chi' k'_\parallel)]\sin[a/2(\eta k_\parallel - \eta' k'_\parallel)] \\
&\times e^{i[x(\eta k_\parallel - \eta' k'_\parallel) + y(\chi k_\parallel - \chi' k'_\parallel) + k_z z + k'_z z']},
\end{aligned} \tag{31}$$

where we have abbreviated

$$\begin{aligned}
\chi &\equiv \cos\phi, \quad \chi' \equiv \cos\phi', \\
\eta &\equiv \sin\phi, \quad \eta' \equiv \sin\phi'
\end{aligned} \tag{32}$$

and immediately taken the parallel coincidence limit $\mathbf{r}'_\parallel \to \mathbf{r}_\parallel$. The perturbative approximation holds as long as both $\Delta\epsilon_c = \epsilon_c(\omega_A) - 1 < 1$ and the dimensions of the object are small compared to the wavelength that corresponds to ω_A [60]. The latter condition can be expressed as $\omega_A a/2\pi \ll 1$. As shown in the below, we take the size of the cube to be equal to $\omega_A z$ (in natural units) so that both of these conditions are satisfied.

The quadruple integrals, (30) and (31), are straightforward to numerically evaluate in ready-made software such as Mathematica or Maple; no specialized numerical techniques are required. Their ease of evaluation arises because the angular integrals are over a finite range and the $k_\parallel$ integrals are exponentially damped at infinity. We present a selection of results of this numerical study in Figs. 4 and 5. We note, in particular, that Fig. 5 shows the highly nontrivial position dependence of the decay rate; for example, the decay rate can be enhanced or suppressed (relative to the value near a bare half-space) depending on the precise position of the atom in the plane above the cube. This is in qualitative agreement with the results obtained in [34] via a different method.

IV. CASIMIR-POLDER POTENTIAL OF A FINITE GRATING

A. Background and motivation

We now turn our attention to a more complex but experimentally relevant situation, namely, the CP potential of an atom near a surface, as first described in [2]. The CP

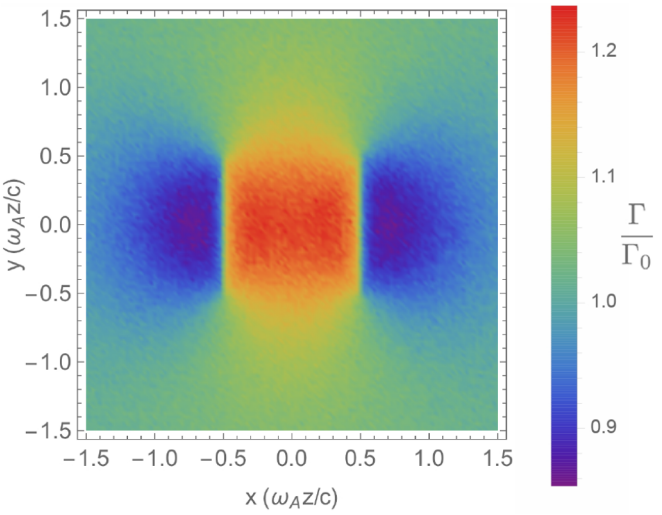

FIG. 5. (Color online) Normalized decay rate for an x-polarized atom at a distance $0.01a$ above a cube of side length $a = 1$ (in dimensionless units $\omega_A z/c$) and dielectric constant $\epsilon_c(\omega) = 1.8$ deposited on a perfectly reflecting half-space. The decay rate is expressed in units of the decay rate at the same distance above the "bare" perfectly reflecting half-space (i.e., that with no cubic deposition).

potential results from the modification of the level structure of a polarizable atom by a surface-dependent quantized field; it is the surface-dependent version of the Lamb shift. The resultant force has been measured to a high precision [67] and is of increasing importance in emerging quantum technologies [68]. The calculation is inherently more complicated than that for the decay rate in Sec. III A. As we shall see, this is largely because the potential depends on a sum over all photon frequencies, rather than being determined by a specific transition frequency like the decay rate. An additional complication is that calculation of a CP potential involves subtraction of the contribution of the homogeneous part of the Green's function at each particular point in order to extract a geometry dependence. This is necessary because, unlike the decay rate, evaluation of a CP potential in free space (i.e., the Lamb shift) requires a completely different full field-theoretic approach. As detailed in Sec. I, care must be taken with CP potentials in this Born-series approach because of the interplay between this subtraction of a homogeneous part and the perturbative approximation.

We calculate the CP potential in vacuum near an N-grooved finite grating, like that shown in Fig. 6. This choice is motivated by the structures used ongoing experiments in atom optics and matter-wave interferometry such as [35] and [69]. There is a body of existing literature on Casimir and CP forces near periodic gratings [25–27], however, these works take advantage of the Bloch theorem and so are only strictly applicable to infinite, precisely periodic gratings, which are not necessarily good approximations to real experiments. In fact, as we will see later, nontrivial behavior of the CP potential occurs *outside* the immediate vicinity of the grating, which of course cannot be seen if the grating is assumed to be infinite.

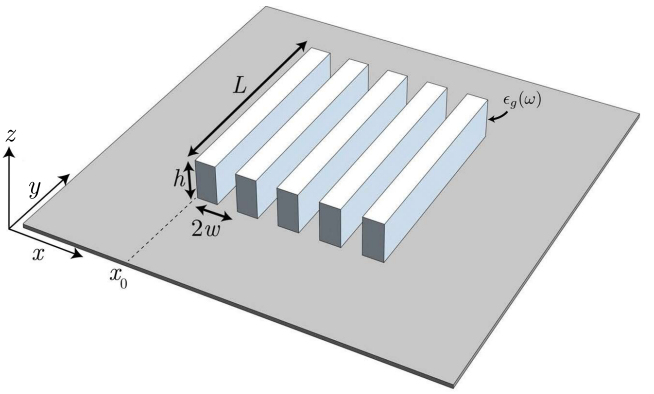

FIG. 6. (Color online) Geometry of the finite grating considered here. Just as for the cubic deposition shown in Fig. 3, the substrate can be made of any desired material; again, the only restriction on the system is that the grating material must be weakly dielectric. While our method works for any number of grooves N, we choose $N = 5$ here and throughout as shown.

B. Expressions for the Casimir-Polder potential

The CP potential $U_{\rm CP}$ for an isotropically polarizable atom at position $\mathbf{r}_A = (x_A, y_A, z_A)$ in a region with a *scattering* EM Green's function $\mathbf{G}$ may be written in terms of an integral over the complex frequency ξ as [51,55]

$$U_{\rm CP}(\mathbf{r}_A) = \frac{1}{2\pi}\int_0^\infty d\xi\, \xi^2 \alpha(i\xi) \mathrm{Tr}\, \mathbf{G}(\mathbf{r}_A, \mathbf{r}_A, i\xi), \tag{33}$$

where α is the polarizability of a ground-to-excited atomic state transition of frequency ω_{ij} and dipole moment d_{ij} and is given by

$$\alpha(\omega) = \frac{2}{3}\lim_{\varepsilon\to 0}\frac{\omega_{ij}|d_{ij}|^2}{\omega_{ij}^2 - \omega^2 - i\omega\varepsilon}, \tag{34}$$

where ε is a real infinitesimal [70] related to the line width of the atomic state [71]. The Green's function is to be taken with both spatial arguments equal to the position $\mathbf{r}_A$ of the atom; this is to be understood as a limiting value. Just as in the decay rate calculation in Sec. III A, we use a selection of standard results as points of comparison for later results. The first of these is the CP potential at a distance z_A from a perfectly conducting plane in the nonretarded regime, This regime is where the round-trip time for a photon to travel from the atom to the surface and back is much shorter than the time scale associated with the atomic frequency. In other words, it is the small-distance approximation if the atomic transition frequency is assumed to be a fixed constant. The well-known result in this regime is [2]

$$U_{\rm CP0}(\omega_A z_A \ll 1) = -\frac{|d_{ij}|^2}{48\pi z_A^3}. \tag{35}$$

The second quantity we use as a comparison is the force that an atom in this potential experiences, namely,

$$F_{\rm CP0}(\omega_A z_A \ll 1) = -\frac{\partial}{\partial z_A} U_{\rm CP0}(\omega_A z_A \ll 1)$$
$$= -\frac{|d_{ij}|^2}{16\pi z_A^4}, \tag{36}$$

which is a statement of the well-known CP force of attraction between a polarizable atom and surface, in this case in the nonretarded regime and for a perfectly conducting material.

Equation (8) tells us that the Green's function that encodes the behavior of the EM field near the grating is given by the sum of two terms: $\mathbf{W}^{\mathrm{HS}}$, which describes the unperturbed half-space; and $\Delta\mathbf{W}^{\mathrm{HS}}(\mathbf{r},\mathbf{r}',\omega)$, which describes the correction resulting from deposition of the grating on its surface. The CP potential, (33), requires the use of a scattering Green's function. Since the whole Green's function $\mathbf{W}$ is linear in its two contributions $\mathbf{W}^{\mathrm{HS}}$ and $\Delta\mathbf{W}^{\mathrm{HS}}(\mathbf{r},\mathbf{r}',\omega)$, it suffices to find the scattering parts $\mathbf{G}^{\mathrm{HS}}$ and $\Delta\mathbf{G}^{\mathrm{HS}}(\mathbf{r},\mathbf{r}',\omega)$ of these two contributions separately, which together give the scattering Green's function $\mathbf{G}$. Also, the linearity of the CP potential in the scattering Green's function means that we can find the contributions from the two scattering parts separately. We confine ourselves to the most physically relevant region, $z,z' > 0$, meaning that the subtraction of a homogeneous part is achieved by setting all reflection coefficients in the Green's function to 0 and subtracting the resulting quantity. For the unperturbed part $\mathbf{G}^{\mathrm{HS}}$ we have

$$\mathbf{G}^{\mathrm{HS}}(\mathbf{r},\mathbf{r}',\omega) = \mathbf{W}^{\mathrm{HS}}(\mathbf{r},\mathbf{r}',\omega) - \mathbf{W}^{\mathrm{HS}}_{R_\sigma\to 0}(\mathbf{r},\mathbf{r}',\omega), \quad (37)$$

where $\mathbf{W}^{\mathrm{HS}}_{R_\sigma\to 0}(\mathbf{r},\mathbf{r}',\omega)$ coincides with the Green's function of free space since the region near the grating is assumed to be a vacuum.

The scattering part of the Green's function correction, (14), is obtained by subtracting the portion that remains when setting all reflection coefficients to 0. Consequently, isolating the scattering part $\Delta\mathbf{G}^{\mathrm{HS}}(\mathbf{r},\mathbf{r}',\omega)$ of $\Delta\mathbf{W}(\mathbf{r},\mathbf{r}',\omega)$ is trivial because of the way it is stated in Eq. (14): all one needs to to is remove the term independent of reflection coefficients, giving

$$\Delta\mathbf{G}^{\mathrm{HS}}_{ij}(\mathbf{r},\mathbf{r}',\omega) = \int_V d^3\mathbf{s}\int d^2\mathbf{k}_\parallel \int d^2\mathbf{k}'_\parallel P\Big[K^{\mathrm{TETM}}_{ij} R_{\mathrm{TE}} R_{\mathrm{TM}} + \sum_\sigma \left(K^{\sigma}_{ij} R_\sigma + K^{\sigma\sigma}_{ij} R^2_\sigma\right)\Big], \quad (38)$$

with the matrix elements K_{ij} listed in the Appendix. Now that we have the Green's function correction, (38), we can find the correction to the CP potential resulting from the deposition of the grating on the half-space from

$$\Delta U_{\mathrm{CP}}(\mathbf{r}_{\mathrm{A}}) = \frac{1}{2\pi}\int_0^\infty d\xi\, \xi^2 \alpha(i\xi)\mathrm{Tr}\,\Delta\mathbf{G}(\mathbf{r}_{\mathrm{A}},\mathbf{r}_{\mathrm{A}},i\xi). \quad (39)$$

C. Grating results and discussion

The volume integral describing the N-grooved grating shown in Fig. 6 is

$$\int_V d^3\mathbf{s} \to \sum_{n=0}^{N-1}\int_{x_0+2nw}^{x_0+(2n+1)w} ds_x \int_{-L/2}^{L/2} ds_y \int_0^h ds_z, \quad (40)$$

with $x_0 = -w(N - 3/4)$ if the grating is such that the center of the base of the middle groove is at $s_x = 0$. For simplicity, the half-space is taken as perfectly reflecting, and the grating as nondispersive, $\epsilon_g(\omega) = \epsilon_g$, with $\epsilon_g - 1 < 1$. We choose $N = 5$, which corresponds to the grating shown in Fig. 6. The atom's polarizability is taken to be isotropic. Using the volume elements, (40), the integrals over $\mathbf{s}$ in (39) become elementary. This leaves integrals over $k_\parallel$, $k'_\parallel$, ξ, θ, and θ', which may be evaluated numerically. Just as for the decay rate calculation in Sec. III A, the integration is significantly simplified by the fact that the integrals over θ and θ' are both over the finite region $0\ldots\pi/2$, and the remaining integrals are all exponentially damped. A selection of results is shown in Figs. 7 and 8 The results for the CP potential directly above the grating show qualitative agreement with the infinite grating considered in [25], where it was observed that the potential is reduced between the grooves and enhanced above them,compared to the planar result. However, our results are not directly quantitatively comparable with [25] because the choices of materials made there are not consistent with our perturbative expansion. Our results for the region "outside" the grating were of course not seen even qualitatively in [25] due to that work's assumption of an infinite grating. Here we have relaxed this assumption and found that the periodicity of the CP potential continues laterally past the end of the grating, which, to our knowledge, is previously unseen in this context.

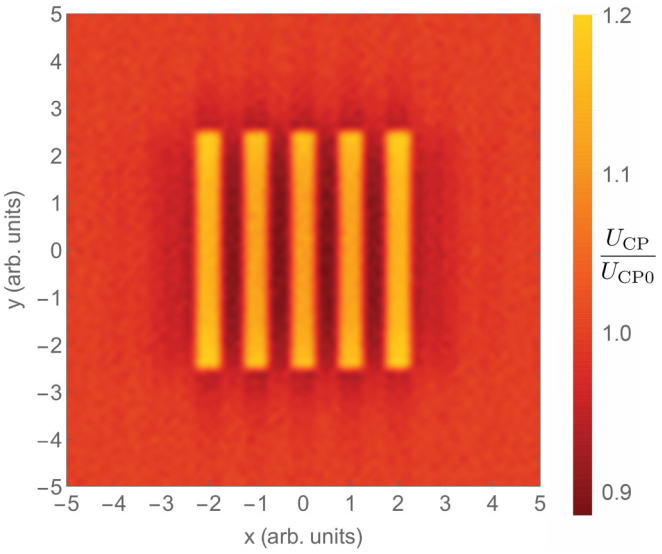

FIG. 7. (Color online) Nonretarded Casimir-Polder potential a distance $z = 1.01h$ from a grating of height h as shown in Fig. 6. The potential is shown in units of the perfect reflector potential, (35), which is the potential if the grating had not been deposited on the half-space. All length scales in the problem can be expressed in terms of a reference length which cancels out (in the nonretarded regime) when normalizing to the bare perfect reflector result. Thus, the units on both axes of the above plot are arbitrary; in other words, the result remains valid whatever unit is assigned to the x and y axes as long as the nonretarded approximation holds. The parameters describing the grating are $h = 1$, $w = 1$, and $L = 5$, in the same units as the x and y axes. The dielectric constant is $\epsilon_g = 1.8$. Almost invisible in this figure is a suggestion of interesting behavior "outside" the grating along the x axis; this is shown in detail in Fig. 8.

V. CONCLUSIONS

In this paper we have considered some aspects of quantum electrodynamics near a surface with arbitrarily shaped features deposited on it. The main general result is the Green's function, (14), for the perturbed half-space, which was calculated

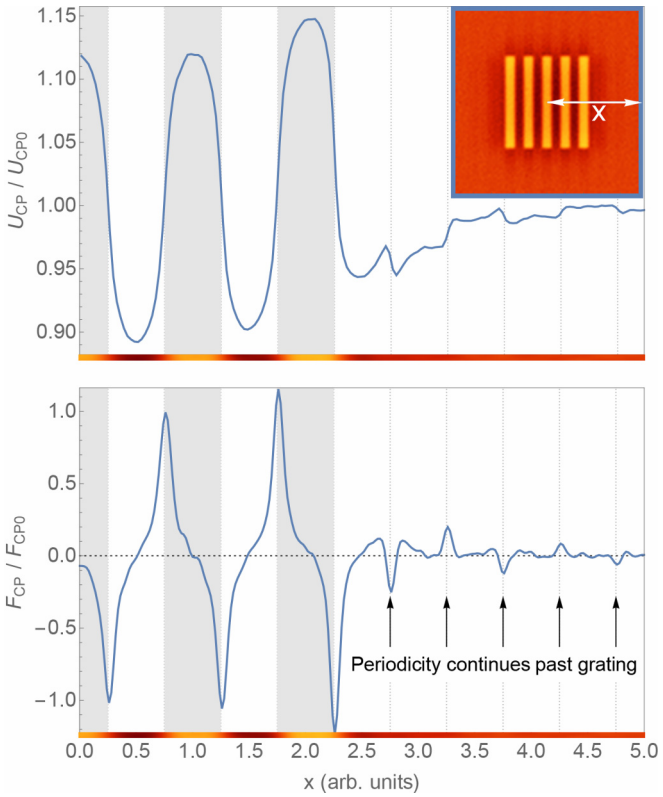

FIG. 8. (Color online) Top: Potential U_{CP} near the grating shown in Fig. 6. As in Fig. 7 the potential is plotted in units of its value U_{CP0} [Eq. (35)] near a simple planar perfect reflector, and all the parameters are the same as for Fig. 7, which is reproduced as the inset and schematically on the horizontal axes. Bottom: Lateral (x-directed) force F_{CP} near the grating shown in Fig. 6 for the same parameters used in Fig. 7. In the same spirit as the other plots, we normalize to what the force would have been if the grating were not present, but the lateral force without the grating would of course be 0. For this reason we use the (constant) perpendicular force, (36), as a unit instead.

using a Born-series expansion. As an example we then have investigated the decay rate of an atom near a cube deposited on a half-space, finding the rich position dependence shown in Fig. 5. Finally, we have presented the CP potential of a finite grating deposited on a substrate and demonstrated the previously unseen quality that the lateral periodicity of the potential can continue beyond the grating, as shown in Fig. 8. The Green's function, (14), can be used to calculate quantum electrodynamical quantities near a half-space with *any* small deposition on it, so the work presented here should have applications in a variety of ongoing and planned experiments [35,68,69].

ACKNOWLEDGMENT

It is a pleasure to thank the UK Engineering and Physical Sciences Research Council Doctoral Prize Fellowship (EPSRC) for financial support.

APPENDIX: GREEN'S FUNCTION MATRIX ELEMENTS

There are five terms in Eq. (14), each of which is one of two 3×3 matrices (one for each choice of $r_z \lessgtr s_z$), giving a total of 90 matrix elements that we, in principle, need to calculate. However, there are various constraints that reduce this number significantly. First, some matrix elements are not independent due to the xy symmetry of the half-space. In particular,

$$\begin{aligned} K^{\tau}_{yy\lessgtr} &= K^{\tau}_{xx\lessgtr}(k_x \leftrightarrow k_y),\\ K^{\tau}_{yz\lessgtr} &= K^{\tau}_{xz\lessgtr}(k_x \leftrightarrow k_y),\\ K^{\tau}_{zy\lessgtr} &= K^{\tau}_{zx\lessgtr}(k_x \leftrightarrow k_y),\\ K^{\tau}_{yx\lessgtr} &= K^{\tau}_{xy\lessgtr}, \end{aligned} \tag{A1}$$

where $\tau = (\mathrm{TE}, \mathrm{TM}, \mathrm{TETE}, \mathrm{TMTM}, \mathrm{TETM})$. This restriction reduces the number of required matrix elements by

$$(4 \text{ constraints }) \times (5 \text{ different } \tau) \times (2 \text{ for } r_z \lessgtr s_z) = 40,$$

leaving a total of 50. This number can be further reduced by noting that the definition of TE modes is that they have no electric field in the z direction, which ultimately means that any matrix element for TE polarization where at least one index is z is in fact identically 0,

$$\begin{aligned} K^{\mathrm{TE}}_{xz\lessgtr} = K^{\mathrm{TE}}_{zx\lessgtr} = K^{\mathrm{TE}}_{zz\lessgtr} = 0,\\ K^{\mathrm{TETE}}_{xz\lessgtr} = K^{\mathrm{TETE}}_{zx\lessgtr} = K^{\mathrm{TETE}}_{zz\lessgtr} = 0, \end{aligned} \tag{A2}$$

and similarly,

$$K^{\mathrm{TETM}}_{xz\lessgtr} = K^{\mathrm{TETM}}_{zx\lessgtr} = K^{\mathrm{TETM}}_{zz\lessgtr} = 0, \tag{A3}$$

which together reduce the required number by 18, leaving $90-40-18=32$ matrix elements to calculate, which can be partitioned into two groups of 16, where each group corresponds to one choice of $r_z \lessgtr s_z$. We now simply list these matrix elements, which are obtained by application of the differential operators, (10), to the functions $F^{\sigma}(z,z')$ given by Eq. (11). For $r_z > s_z$ the matrix elements representing coefficients of terms linear in the reflection coefficients are

$$\begin{aligned} K^{\mathrm{TE}}_{xx>} &= e^{-2ik_z s_z}\omega^2 k_y'^2\left(k_x^2k_z^2 + k_y^2\omega^2\right) + \text{primed},\\ K^{\mathrm{TE}}_{xy>} &= e^{-2ik_z s_z}k_x k_x' k_y k_y'\omega^2 k_\parallel^2 + \text{primed},\\ K^{\mathrm{TM}}_{xx>} &= -e^{-2ik_z s_z}k_x'^2 k_z'^2\left(k_x^2k_z^2 + k_y^2\omega^2\right) + \text{primed},\\ K^{\mathrm{TM}}_{xy>} &= e^{-2ik_z s_z}k_\parallel^2 k_x' k_y k_y' k_x k_z'^2 + \text{primed},\\ K^{\mathrm{TM}}_{xz>} &= e^{-2ik_z s_z}k_x k_x' k_z k_z' k_\parallel^2 k_\parallel'^2 - \text{primed},\\ K^{\mathrm{TM}}_{zx>} &= -e^{-2ik_z s_z}k_x k_x' k_z k_z' k_\parallel^2 k_\parallel'^2 - \text{primed},\\ K^{\mathrm{TM}}_{zz>} &= e^{-2ik_z s_z}k_\parallel^4 k_\parallel'^4 + \text{primed}, \end{aligned} \tag{A4}$$

where "primed" is shorthand for the quantity that precedes it with $\mathbf{k}\to\mathbf{k}'$ and $\mathbf{r}\to\mathbf{r}'$, with the latter replacement being relevant only for $r_z < s_z$ as we shall see. Continuing, the $r_z > s_z$ matrix elements representing coefficients of terms quadratic in particular reflection coefficients are

$$\begin{aligned} K^{\mathrm{TETE}}_{xx>} &= k_y^2 k_y'^2\omega^4, \quad K^{\mathrm{TMTM}}_{xx>} = k_x^2 k_x'^2 k_z^2 k_z'^2,\\ K^{\mathrm{TETE}}_{xy>} &= k_x' k_x k_y' k_y\omega^4, \quad K^{\mathrm{TMTM}}_{xy>} = k_x k_x' k_y k_y' k_z^2 k_z'^2,\\ K^{\mathrm{TMTM}}_{xz>} &= k_x k_x' k_z k_z' k_\parallel^2 k_\parallel'^2, \quad K^{\mathrm{TMTM}}_{zx>} = k_x k_x' k_z k_z' k_\parallel^2 k_\parallel'^2,\\ K^{\mathrm{TMTM}}_{zz>} &= k_\parallel^4 k_\parallel'^4, \end{aligned} \tag{A5}$$

and finally, the coefficients of the terms that mix TE and TM reflection coefficients,

$$K^{\mathrm{TETM}}_{xx>} = -\omega^2\left(k_x^2 k_y'^2 k_z^2 + k_x'^2 k_y^2 k_z'^2\right),$$
$$K^{\mathrm{TETM}}_{xy>} = k_x k_x' k_y k_y' \omega^2\left(k_z^2 + k_z'^2\right). \quad \text{(A6)}$$

For $r_z < s_z$ the entire set of 16 coefficients can be obtained from Eqs. (A4)–(A6) by taking $s_z \to r_z$ (before adding the "primed" parts), so that, for example,

$$K^{\mathrm{TM}}_{zz<} = (e^{-2ik_z r_z} + e^{-2ik_z r_z'})k_\parallel^4 k_\parallel'^4. \quad \text{(A7)}$$

We have now completely specified all terms in (14).

[1] H. B. Casimir, Proc. K. Ned. Akad. Wet **51**, 150 (1948).
[2] H. B. G. Casimir and D. Polder, Phys. Rev. **73**, 360 (1948).
[3] K. H. Drexhage, Prog. Opt. **12**, 163 (1974).
[4] R. R. Chance, A. Prock, and R. Silbey, Adv. Chem. Phys **37**, 1 (1978).
[5] M. S. Yeung and T. K. Gustafson, Phys. Rev. A **54**, 5227 (1996).
[6] S. Scheel, L. Knöll, and D. G. Welsch, Phys. Rev. A **60**, 4094 (1999).
[7] E. Fischbach and N. Nakagawa, Phys. Rev. D **30**, 2356 (1984).
[8] D. G. Boulware, L. S. Brown, and T. Lee, Phys. Rev. D **32**, 729 (1985).
[9] M. Kreuzer and K. Svozil, Phys. Rev. D **34**, 1429 (1986).
[10] M. Kreuzer, J. Phys. A **21**, 3285 (1988).
[11] G. Barton and N. S. J. Fawcett, Phys. Rep. **170**, 1 (1988).
[12] R. Bennett and C. Eberlein, New J. Phys. **14**, 123035 (2012).
[13] R. Bennett and C. Eberlein, Phys. Rev. A **88**, 012107 (2013).
[14] R. Bennett and C. Eberlein, Phys. Rev. A **86**, 062505 (2012).
[15] R. Bennett and C. Eberlein, Phys. Rev. A **89**, 042107 (2014).
[16] M. Donaire, M. P. Gorza, A. Maury, R. Guérout, and A. Lambrecht, Europhys. Lett. **109**, 24003 (2015).
[17] F. S. S. Rosa, D. A. R. Dalvit, and P. W. Milonni, Phys. Rev. A **78**, 032117 (2008).
[18] M. Antezza, L. P. Pitaevskii, and S. Stringari, Phys. Rev. Lett. **95**, 113202 (2005).
[19] D. A. R. Dalvit, P. A. Maia Neto, A. Lambrecht, and S. Reynaud, Phys. Rev. Lett. **100**, 040405 (2008).
[20] P. Milonni, *The Quantum Vacuum: An Introduction to Quantum Electrodynamics* (Academic Press, New York, 1994).
[21] C. Farina, F. C. Santos, and A. C. Tort, Am. J. Phys. **67**, 344 (1999).
[22] B. Derjaguin and I. Abrikosova, Sov. Phys. JETP **3**, 819 (1957).
[23] H. Gies and K. Klingmüller, Phys. Rev. Lett. **96**, 220401 (2006).
[24] P. A. M. Neto, A. Lambrecht, and S. Reynaud, Europhys. Lett. **69**, 924 (2005).
[25] A. M. Contreras-Reyes, R. Guérout, P. A. M. Neto, D. A. R. Dalvit, A. Lambrecht, and S. Reynaud, Phys. Rev. A **82**, 052517 (2010).
[26] A. Lambrecht and V. N. Marachevsky, Phys. Rev. Lett. **101**, 160403 (2008).
[27] J. Lussange, R. Guérout, and A. Lambrecht, Phys. Rev. A **86**, 062502 (2012).
[28] A. Rodriguez, M. Ibanescu, D. Iannuzzi, F. Capasso, J. D. Joannopoulos, and S. G. Johnson, Phys. Rev. Lett. **99**, 080401 (2007).
[29] S. Reynaud, P. A. M. Neto, and A. Lambrecht, J. Phys. A **41**, 164004 (2008).
[30] H. C. Chiu, G. L. Klimchitskaya, V. N. Marachevsky, V. M. Mostepanenko, and U. Mohideen, Phys. Rev. B **80**, 121402 (2009).
[31] F. Intravaia, S. Koev, I. W. Jung, A. A. Talin, P. S. Davids, R. S. Decca, V. A. Aksyuk, D. A. R. Dalvit, and D. López, Nature Commun. **4**, 2515 (2013).
[32] G. Bimonte, T. Emig, and M. Kardar, Phys. Rev. D **90**, 081702 (2014).
[33] R. Messina, D. A. R. Dalvit, P. A. M. Neto, A. Lambrecht, and S. Reynaud, Phys. Rev. A **80**, 022119 (2009).
[34] C. Henkel and V. Sandoghdar, Opt. Commun. **158**, 250 (1998).
[35] C. C. Nshii, M. Vangeleyn, J. P. Cotter, P. F. Griffin, E. A. Hinds, C. N. Ironside, P. See, A. G. Sinclair, E. Riis, and A. S. Arnold, Nature Nanotechnol. **8**, 321 (2013).
[36] S. Y. Buhmann and D. G. Welsch, Appl. Phys. B **82**, 189 (2006).
[37] R. Golestanian, Phys. Rev. A **80**, 012519 (2009).
[38] R. Bennett, Phys. Rev. A **89**, 062512 (2014).
[39] M. Nieto-Vesperinas, *Scattering and Diffraction in Physical Optics* (Wiley, New York, 1991).
[40] D. Lu, J. J. Kan, E. E. Fullerton, and Z. Liu, Nature Nanotechnol. **9**, 48 (2014).
[41] J. M. Elson and R. H. Ritchie, Phys. Rev. B **4**, 4129 (1971).
[42] A. A. Maradudin and D. L. Mills, Phys. Rev. B **11**, 1392 (1975).
[43] M. Nieto-Vesperinas, J. Opt. Soc. Am. **72**, 539 (1982).
[44] P. A. M. Neto, A. Lambrecht, and S. Reynaud, Phys. Rev. A **72**, 012115 (2005).
[45] L. Suresh and J. Y. Walz, J. Colloid Interface Sci. **183**, 199 (1996).
[46] V. B. Bezerra, G. L. Klimchitskaya, and C. Romero, Phys. Rev. A **61**, 022115 (2000).
[47] S. Rytov, Y. A. Krastov, and V. Tatarskii, *Principles of Statistical Radiophysics 3, Elements of the Random Fields* (Springer, Berlin, 1987).
[48] T. Gruner and D. G. Welsch, Phys. Rev. A **53**, 1818 (1996).
[49] H. T. Dung, L. Knoll, and D.-G. Welsch, Phys. Rev. A **57**, 3931 (1998).
[50] R. Matloob, R. Loudon, S. M. Barnett, and J. Jeffers, Phys. Rev. A **52**, 4823 (1995).
[51] S. Scheel and S. Y. Buhmann, Acta Phys. Slovaca Rev. Tutor. **58**, 675 (2008).
[52] T. G. Philbin, New J. Phys. **12**, 123008 (2010).
[53] We work in a system of natural units where the speed of light c, the reduced Planck constant $\hbar$, and the permittivity of free space ϵ_0 are all equal to 1.
[54] The reason for avoiding the standard notation **G** is that we reserve this symbol for the scattering Green's function (consistent with our previous work [38]), as opposed to the whole Green's function. In [38] the whole Green's function **W** was given the more obvious symbol Γ, but here that is reserved for the spontaneous decay rate.
[55] J. M. Wylie and J. E. Sipe, Phys. Rev. A **30**, 1185 (1984).
[56] W. C. Chew, *Waves and Fields in Inhomogeneous Media* (IEEE Press, New York, 1995).

[57] J. Knoester and S. Mukamel, Phys. Rev. A **40**, 7065 (1989).
[58] S. M. Barnett, B. Huttner, and R. Loudon, Phys. Rev. Lett. **68**, 3698 (1992).
[59] T. Kalkbrenner, U. Håkanson, A. Schädle, S. Burger, C. Henkel, and V. Sandoghdar, Phys. Rev. Lett. **95**, 200801 (2005).
[60] R. Carminati and J.-J. Greffet, JOSA A **12**, 2716 (1995).
[61] A. Sentenac and J. J. Greffet, Ultramicroscopy **57**, 246 (1995).
[62] D. Van Labeke and D. Barchiesi, JOSA A **10**, 2193 (1993).
[63] G. Parent, D. Van Labeke, and D. Barchiesi, JOSA A **16**, 896 (1999).
[64] S. Scheel, L. Knöll, D.-G. Welsch, and S. M. Barnett, Phys. Rev. A **60**, 1590 (1999).
[65] W. Vogel and D. Welsch, *Quantum Optics* (Wiley, New York, 2006).
[66] D. Meschede, W. Jhe, and E. A. Hinds, Phys. Rev. A **41**, 1587 (1990).
[67] C. I. Sukenik, M. G. Boshier, D. Cho, V. Sandoghdar, and E. A. Hinds, Phys. Rev. Lett. **70**, 560 (1993).
[68] T. E. Judd, R. G. Scott, A. M. Martin, B. Kaczmarek, and T. M. Fromhold, New J. Phys. **13**, 083020 (2011).
[69] A. Günther, S. Kraft, C. Zimmermann, and J. Fortágh, Phys. Rev. Lett. **98**, 140403 (2007).
[70] The infinitesimal ε should not be confused with the dielectric constant ϵ.
[71] P. W. Milonni and R. W. Boyd, Phys. Rev. A **69**, 023814 (2004).